Transactions of the 15th International Conference on
Structural Mechanics in Reactor Technology (SMiRT-15)
Seoul, Korea, August 15-20, 1999

Three-Dimensional Analysis of Steam/Hydrogen Transport with Catalytic Recombiners in Nuclear Reactor Containments Using the Computer Code GASFLOW.

P. Royl[1], H. Rochholz[1], J. R. Travis[2], G. Necker[3], W. Breitung[1], L. Seyffarth[4] and W. Gehrig[5]

1) Forschungszentrum Karlsruhe, Germany
2) Ing. Büro Du Bois, Pitzer, Travis, Germany
3) Pro-Science, Germany
4) RWE-Energie AG, Germany
5) Gemeinschaftskernkraftwerk Neckar GmbH, Germany

ABSTRACT

The GASFLOW code has been applied for the analysis of the steam/hydrogen distribution with mitigation by catalytic recombiners under conditions of a large break loss-of-coolant accident for 3D containment models of two different types of German pressurized water reactors (PWRs). The contribution describes the developed 3D containment models, the applied concept for recombiner positioning, and it discusses the calculated results in relation to the applied source term which was the same in both containments. It identifies the principal mechanisms that determine the hydrogen mixing in these two containments, and it shows up generic differences to similar simulations performed with lumped parameter codes.

INTRODUCTION

During hypothetical core melt accidents, steam and hydrogen can be released into the containment of pressurized water reactors. Without counter measures, flammable mixtures may form and cause combustion loads that could threaten the integrity of the containment. Such sequences have a very low probability of occurrence and are beyond the design envelope of nuclear power plants. New safety regulations issued in Germany in 1994 request measures for a risk reduction to prevent an early containment failure during such beyond-design sequences. One such measure is the implementation of recombiners for the early catalytic combustion of the released hydrogen to prevent the buildup of detonable hydrogen/air mixtures in the containment atmosphere.

The 3D field code GASFLOW [1] is a joint development of Forschungszentrum Karlsruhe and Los Alamos National Laboratory for the simulation of steam/hydrogen distribution and combustion in complex containment geometries. GASFLOW gives a full solution of the compressible 3D Navier-Stokes equations and has been validated by analysing experiments that simulate the relevant aspects and integral sequences of such accidents. The newly released and validated version 2.1 of GASFLOW has been applied in a mechanistic 3D analysis of steam/hydrogen distribution with mitigation involving a large number of different catalytic recombiners at various locations in two types of spherical PWR containments of German design. The simulations are the first full analyses for quite complex containment models. The results show up some generic differences between similar simulations carried out in parallel by using so-called lumped parameter (LP) models [2] that represent the containment by various control volumes which are interconnected through 1D flow pathes, and they identify the controling generic effects for a scenario with a large-break loss-of-coolant accident (LOCA) in two quite different containment geometries. This contribution summarizes the results from these simulations that are further documented in more detailed reports [3,4]. It describes the 3D containment models, explains the applied concept of recombiner positionning, and discusses the results for the pressure and steam/hydrogen distribution in relation to the applied source term.

CONTAINMENT MODELS

Two large 3D Cartesian geometry models were developed for GASFLOW. Plant A represents a spherical PWR containment of a German pre-Konvoi type, Plant B represents a current German Konvoi type PWR. Both plants have spherical containments that are bounded by a concrete shell with an annular gap of air and a steel shell around a free gas volume of ca. 70,000 m^3 (Fig. 1). GASFLOW simulates the spherical concrete shell as stair-stepped obstacles and the steel shell as stair-stepped walls in a 3D Cartesian mesh using 158,000 cells for plant A and 184,000 computational cells for plant B with an average cell volume between 1.3 and 1 m^3 per cell. The structures inside the steel shell are set up according to the plant layouts by defining obstacles

		Plant A	**Plant B**
Volume	m^3	70,163	69,698
Concrete	m^2	19,851	31,140
in. steel shell	m^2	7,639	7,919

Tab. 1: containment volumes and surfaces

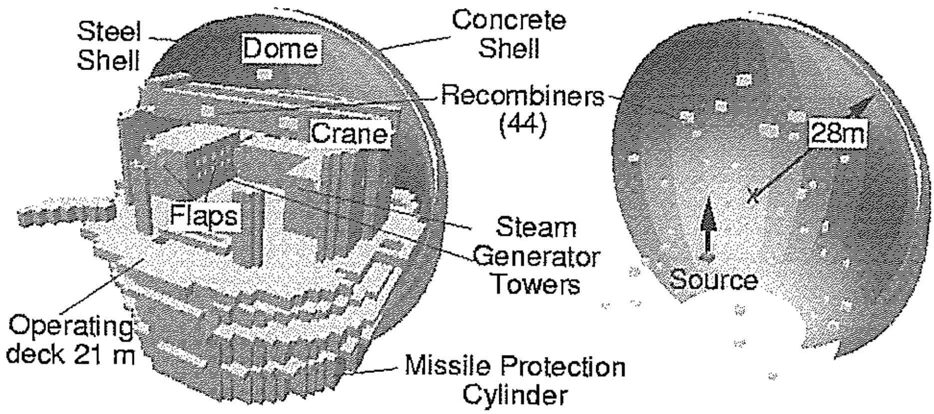

Fig. 1: 3D GASFLOW geometry model for plant A

that occupy full cell volumes, and by putting walls on cell boundaries that block the flow perpendicular to the surface. Obstacles and walls are simulated as heat absorbing structures of either concrete or steel. Their surfaces are adjusted to exactly represent the projected areas on the spherical steel and concrete shell, and they balance in total to the plant data for the internal concrete surfaces and the spherical steel shell surfaces that are given in table 1. The gas flows through the interconnected free cells not occupied by obstacles and through openings that become transiently available when the pressure difference across selected walls (defined as rupture disks or rupture flaps) exceeds a certain value (between 55 and 100 mbars) and causes the removal of this particular wall from the mesh. Figure 1 displays such flaps on the sides of the steam generator towers for plant A. They open connections between the operating room and the so-called component rooms with the pumps and steam generators inside. Steel shell, dome, crane, operating deck and missile protection cylinder are the relevant structures of the operating room visible in Fig. 1. The blowdown source is located in a component room under the left steam generator tower at a low axial location. Its location in the 3D mesh is shown on the right side of the graph which gives the geometry inside the steel sphere without the structures.

The GASFLOW analysis of plant A includes the simulation of mitigation by a total of 44 catalytic hydrogen recombiners that are placed at various locations in the operating and component rooms (Fig. 1). The recombiners are from the NIS type [5]. About 30% of them are attached to the crane support bars and above. Each recombiner is represented by a single fluid cell that is bounded by steel walls on the sides. Gas flow occurs into and through these boxes applying an active ventilation option which determines the flow rate in dependence of the calculated local hydrogen concentration at the box entrance on basis of measured operating data. The recombiners thus operate in a 3D concentration field and reflect all effects from local stratification and sedimentation of gases. An efficiency that is defined pressure-dependent recombines a large fraction of the inflowing hydrogen with oxygen to steam and adds the chemical energy to the gas flow, so that colder gases with hydrogen enter the boxes and hot gases of steam, nitrogen, and oxygen with only some residual amounts of hydrogen leave the boxes. For the NIS recombiners, gases leave the boxes in vertical flow. The analysis of plant B simulates 62 recombiners of the Siemens type [5] that are closed at the top and open on the sides so that hot gases leave the boxes in horizontal flow. The GASFLOW modeling of the Siemens type recombiner boxes was validated with the successful analysis of the Battelle recombiner tests GX4, GX6 and GX7 [6], and for the NIS type recombiners with the analysis of the Battelle test MC3 [7].

RESULTS

The investigated scenario was a large-break LOCA at a low release location from a rupture of the pressure relief line from the hot leg of the primary loop to the pressurizer (surge-line LOCA). The same source was applied in the analysis of plants A and B. It was taken from a MELCOR analysis of this accident [8] and covered the in-vessel phase of this scenario with a total problem time of 7000 s. In the blowdown phase (first 700 s) a two phase mixture of 462 tons of water and 39 tons of steam gets injected. Isenthalpic expansion to the transient containment pressure adds another 50 tons of steam. The relocation of water and steam is considered in a single flow field using a homogeneous equilibrium model, from which the water is parametrically removed with a time constant of 100 s after the achievement of thermal equilibrium between water and steam. Mass and energy of the rained out water are balanced. They could be applied for the simulation of sumps, but were neglected in this analysis. Another 50 tons of superheated steam are released after the blowdown with peak temperatures above 1000 K. Hydrogen release starts after 1500 s. Alltogether 531 kg of hydrogen are added of which 120 kg are entered during a strong release peak at 5932 s due to an enhanced steam/zirconium reaction after the failure of the core support. Volatile fission products (Xenon) are also released. They carry a total decay heat of 8 MW which is released volumetrically dependent on the local Xenon density.

The applied steam/hydrogen release rates are displayed in Fig. 2 together with the calculated pressure transients from GASFLOW for plants A and B. Isenthalpic expansion of the blowdown source leads to an early initial pressure peak of nearly 4 bars in both containments. The further pressure development is controlled by steam condensation and release. Both containments have the same free gas volume of 70,000 m^3. But because plant A is less compartmentalized than plant B and has 30% less concrete surfaces, the pressure decays less rapidly than in plant B after the blowdown, and it increases more

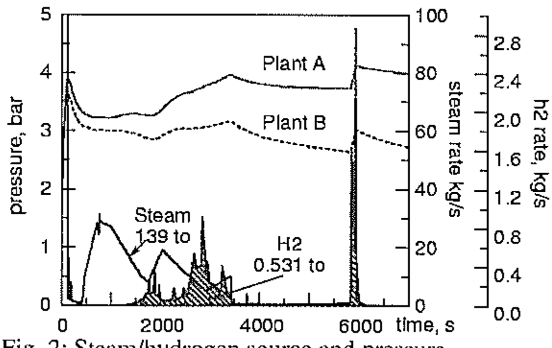

Fig. 2: Steam/hydrogen source and pressure

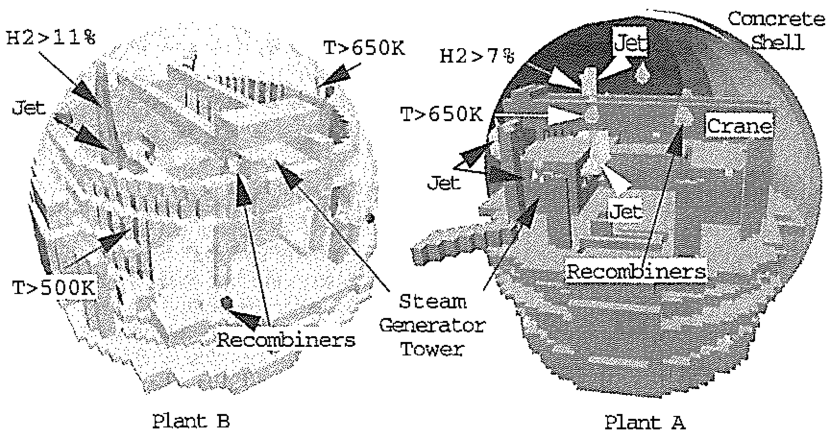

Fig. 3: Hydrogen source jets, stratified clouds and recombiner exhaust plumes, KISMET [11] snapshot of GASFLOW results at end of H2 injection (5932 s)

during the further steam/hydrogen release again reaching 4 bars at the end in plant A compared to 2.4 bars in plant B. Pressure waves open most flaps and rupture disks during the first 0.5 s of the blowdown.

The released source gases of steam and hydrogen form a buoyant jet that rises through the steam generator tower above the source. The gas enters the operating room through the failed rupture disks and flaps in the steam generator tower. The openings from the failed rupture disks, which are on the roofs of the steam generator towers in plant B, allow a direct axial expansion of the buoyant source jet into the dome. In plant A the failed flaps are on the sides of the steam generator towers. The gas from the source jet also rises into the steam generator tower and gets injected horizontally from all sides and forms four fingers which rapidly extend deeply into the dome. Figure 3 shows the calculated buoyant source jets in the dome that result in Plant B (11 vol% H2) and plant A (7 Vol%H2) during the last rapid steam/hydrogen release after core support failure at 5932 s. The calculation of these jets has a good validation basis. GASFLOW could successfully predict such buoyant source jets in the blind pre-calculation of the Battelle Hyjet Helium injection test JX7 [9] and in the analysis of the Canadian Whiteshell tests with little sensitivity to the applied mesh sizes [10]. The snap shots in Fig. 3 also show recombiners higher up in the containment

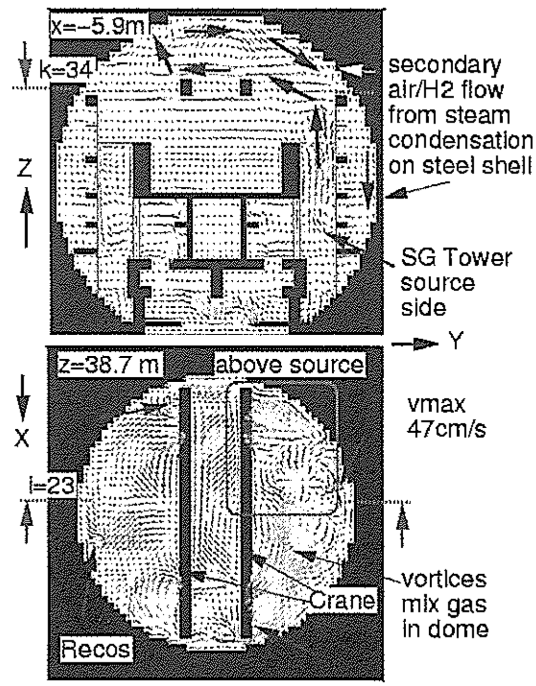

Fig. 4: Vortex mixing in the dome and sedimentation flow in plant B at 5932 s

with pronounced hot exhaust gases (T>650K). They have little impact on the flow field and are outside the source jet in a stratified region built up after the first phase of the steam hydrogen release, while the recombiners at a lower location on the operating deck and away from the source side tower don't yet see much hydrogen at this time. The stratified region in the dome is displayed for plant B as transparent cloud (T>500K).

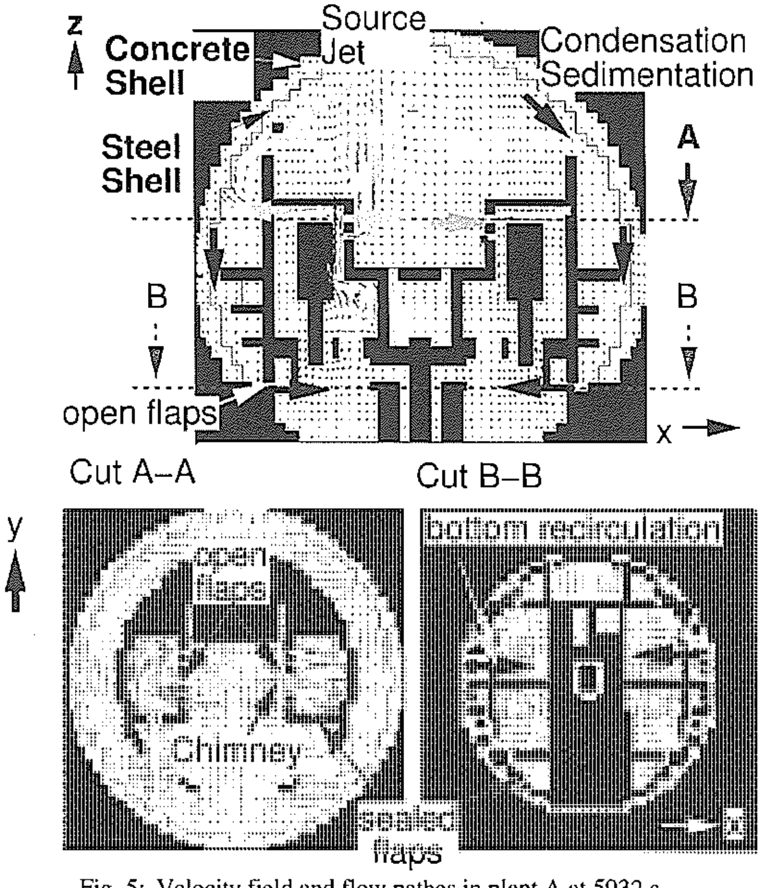

Fig. 5: Velocity field and flow pathes in plant A at 5932 s

The rising source jets after the strong hydrogen release are deflected in the dome near the sphere, spread out to the side, mix within 200 s due to the vortices calculated in GASFLOW as the result of Taylor instabilities and flow diversions in the dome (Fig. 4) and contribute to the formation of a temporarily stratified cloud in the dome. On a larger time scale a secondary flow develops in a thin layer around the condensing structures when steam condensation locally leads to a dried gas with a larger hydrogen and air volume fraction and to a layer with an increased average molecular weight in which this gas sinks down along the cooled structures. This so-called condensation sedimentation effect homogenizes the stratified atmosphere in a "wet" scenario with steam. Due to the smaller structure surfaces of plant A it develops more slowly than in plant B but ultimately it is the same mechanism that is responsible for the atmospheric mixing.

Besides the spreading out of the source jet through the source side steam generator into the dome, GASFLOW also shows the buildup of a temporary circulation from a chimney effect between the steam generator towers which are heated differently on the source side and away from the source with gas flowing from the hot tower into the colder tower on the other side (see cut A-A in Fig.5). A bottom-recirculation also develops through the opened flaps on the low level in cut B-B (Rohrkanal). There are significant asymmetries involved in these circulations due to a smaller failure fraction of the flaps away from the source. Parametric variations with sealed exits in the steam generator tower away from the source and sealed openings for the re-circulation in the bottom region show that these circulations do speed up the mixing for a certain time, but that they don't contribute much to the homogenization on a larger time scale which is controled by the condensation sedimentation effect. The 3D GASFLOW results for the time development of the hydrogen and steam volume fraction and the gas temperatures in the dome

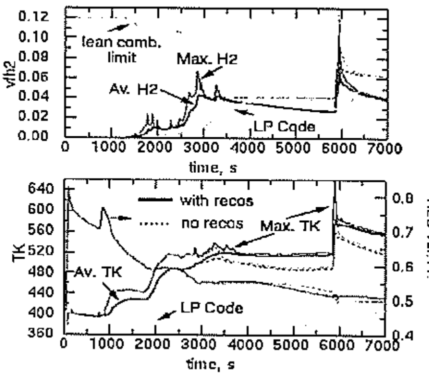

Fig. 6: Hydrogen/steam vol. fractions and temperatures in the dome of plant B

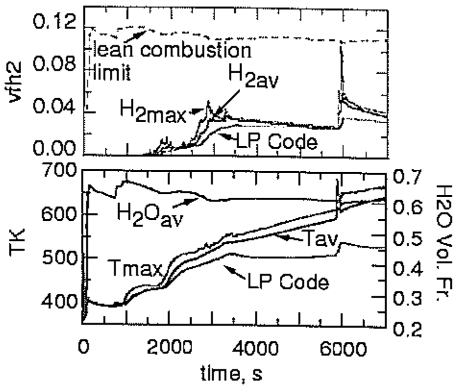

Fig. 7: Hydrogen/steam vol. fractions and temperatures in the dome of plant A

of plants A and B have been averaged for a control volume of ca. 2000 m^3 at the top of the dome which is characteristic for a control zone of the dome in a lumped parameter model of such containment, and which comprises ca. 1500 computational cells in GASFLOW. Figures 6 and 7 display these results for plants B and A. They also include the time dependent local peak hydrogen concentration and temperature occurring in the jets extending into this dome zone. For plant B the dashed lines also give the results of the same simulation without recombiners. The average H2 concentration with recombiners is 4% at the end after going through a maximum of 9% during the last hydrogen injection. The average H2 volume fraction in the dome reaches 3.5 % in plant A at 7000 s after going through a maximum of 6%. Because of the higher steam content and containment pressure it is lower in plant A inspite of an overall higher H2 inventory calculated in plant A due to a slower H2-removal with the installed NIS recombiners. The local peak H2 concentrations in Figs. 6 and 7 significantly exceed the average concentrations during the two periods of H2 injection when the source jets penetrate into the dome. Mixing from vortex formations dilutes the jets within some hundred seconds after each injection period so that the peak and average H2-concentrations merge in the considered dome regions of plants A and B. The Peak H2 concentrations reach maxima of 11% and 10.5% for plant B and plant A. The lean H2-combustion limit [11] in plant B is around 9 Vol% at this time for the steam concentration of 50 Vol% (Fig. 6), and for some 10 s the source jet that extends into the dome of plant B becomes flammable. Plant A has a higher lean H2-combustion limit around 11% (Fig.7). The dome atmosphere has 60 Vol% steam and is inerted enough that the source jet can never become flammable. The local peak and the average gas temperatures in the dome merge rapidly in plant B due to the mixing after each injection period. Temperatures in plant B reach peak values of 640 K and end values of 560 K. In plant A a high temperature zone develops at the top. Hot exhaust plumes from the recombiners, the decay heat from the volatile fission products that stratify together with the hydrogen and a generally reduced structure cooling effect contribute and increase the dome temperatures to 40 K higher peak gas temperatures at the end.

It is difficult to predict such local effects with LP codes even if they represent the containment by a large number of control zones. Their equations don't carry information on the 3D momentum flow which is fully conserved in GASFLOW. The integration effect of the dome control volume allows only for a relatively slow increase of temperatures and concentrations and doesn't reflect the additional heating from the source jet and the fission products which it transports. The simulation of superheated steam together with vaporizing films on the structure in the LP results from Fig. 6 additionally delays the temperature increase in this large control volume. Although LP codes will calculate similarly mixed conditions at the end, they cannot conservatively predict the heterogeneous states occurring during the transition to these mixed states.

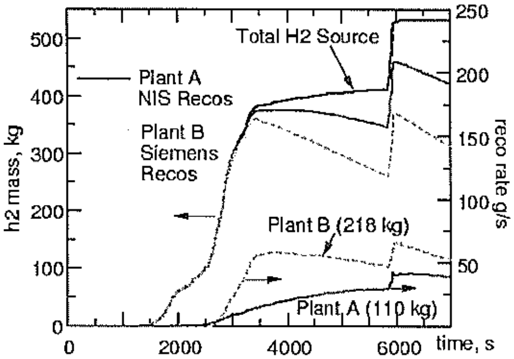

Fig. 8: Hydrogen inventories and recombination rates for analyzed recombiner concepts in plants A and B

With the simulated arrangement of the NIS and of the Siemens recombiners in plants A and B GASFLOW predicts an overall hydrogen removal of 20% and 40%, respectively (Fig. 8). The NIS recombiners with granulate catalysts have a higher heat capacity, start somewhat slower, and respond with larger inertia to transient loadings with hydrogen, so that they need more time in the defined arrangement for removing the same amount of hydrogen.

CONCLUSIONS

The GASLFOW simulations of this scenario with a large break LOCA demonstrate a strong steam inertization in both containments. During the release phases with steam and hydrogen they predict the transient formation of a buoyant jet that extends from the source up through the steam generator towers into the dome. But there is only a short phase in which locally flammable gas mixtures develop in the dome. Vortices formed from Taylor instabilities rapidly dilute the source jet and the regions in which it is flammable. A larger stratified cloud that is inflammable forms in the dome from which a hydrogen/air mixture sinks down in a secondary flow near the structures due to the steam condensation that becomes the major mechanism for homogenizing the temporarily stratified hydrogen. This sedimentation occurs on a larger time scale in plant A which is a more open containment with smaller structure surfaces and heat capacities. Larger volume fractions of steam, reduced hydrogen volume fractions, a higher containment pressure and higher gas temperatures in the dome are the principal differences between the GASFLOW simulations for plants A and B, which are both controlled by the same mechanisms. The hydrogen recombination rate determined from the 3D concentration field is higher in the dome for some time but becomes more and more homogeneous as the hydrogen becomes mixed throughout the containment. This homogeneous removal of hydrogen is well predicted also with simple lumped parameter models which at the end predict a similar integral hydrogen removal as GASFLOW with an overall hydrogen removal fraction at 7000 s of 20% and 40% for plants A and B, respectively. The principal difference is that the 3D GASFLOW simulation describes all mixing mechanisms and flow pathes with a full set of mass, energy, and momentum equations. This resolves all heterogeneous states in between and confirms that the final homogeneous conditions are achieved without the occurrence of intermediate states in which combustions could develop a load potential. On a larger time scale the analyzed mitigation concept with catalytic recombiners of the Siemens and of the NIS type is demonstrated as an effective measure that prevents the formation of combustible mixtures during the ongoing slow deinertization process from steam condensation. The installation of the recombiners is therefore an efficient measure for a further reduction of the hydrogen risk.

ACKNOWLEDGEMENTS

This work was done with support from the German utitlity group VGB. The authors also want to thank Mr. Rohde, Sonnenkalb, and Tiltmann from GRS-Köln for providing the source data from their MELCOR analysis also Mrs. Preusser, Mr. Saal and Klimmt from Siemens, KWU for giving valuable informations for the development of the containment models. Dr. Baumann from FZK is acknowledged for carefully reading this manuscript.

REFERENCES

1. J. R. Travis, J. W. Spore, P. Royl, G. Necker:"Theoretical and Computational Models of the GASFLOW-II Code", These proceedings
2. H. Karwat, et al.:"State of the Art Report on Containment Thermal-Hydraulics and Hydrogen Distribution", Report NEA/SEN/SIN(98) , Paris, 1998
3. P. Royl, H. Rochholz, W. Breitung, J. R. Travis, G. Necker, A. Veser, Report FZKA-6282
4. P. Royl, H. Rochholz, G. Necker, J. R. Travis, Report FZKA-6283
5. K. Fischer:"Qualification of a Passive Catalytic Module for Hydrogen Mitigation", Nuclear Technology Vol. 112, Oct. 1995
6. P. Royl, J. R. Travis, W. Breitung, L. Seyffarth:"Simulation of Hydrogen Transport with Mitigation Using the 3D Field Code GASFLOW", ISBN 0-89448-624-1, Orlando 1997
7. P. Royl, J. R. Travis, E. A. Haytcher, and H. Wilkening, "Analysis of Mitigating Measures during Steam/Hydrogen Distributions in Nuclear Reactor Containments with the 3D Field Code GASFLOW," AECL-11762, NEA/CSNI/R(96)8, Winnipeg 1996
8. M. Sonnenkalb: "Unfallanalysen für DWR mit dem Integralcode MELCOR 1.8.3", GRS-A-2579, June 1998
9. T. Kanzleiter, H. Holzbauer, K. Fischer, M. Geiß, W. Häfner:"Hyjet/Pacos-Versuche im Modellcontainment", Abschlußbericht BF-R40.075-01, Dezember 1996, gefördert durch Bundesministerium für Bildung, Wissenschaft, Forschung und Technologie unter Förderkennzeichen: 15NU0962
10. W. Baumann: "Effects of Oversized Jet Flow Areas in GASFLOW analysis Investigations of Canadian Gas Mixing Tests", 6. Fortschrittsbericht Zusammenarbeit FZK/EVU/Siemens, März 1999
11. Z. M. Shapiro, T. R. Moffette:"Hydrogen Flammability Data and Application to PWR Loss-of-Coolant Accident",WAPD-SC-545, Bettis Plant, September 1957
12. U. Kühnapfel et al., FZK-Nachrichten 2-3/1996